Quaternary Geochronology 20 (2014) 1–7

Contents lists available at ScienceDirect

Quaternary Geochronology

journal homepage: www.elsevier.com/locate/quageo

Short communication

Conversion of GISP2-based sediment core age models to the GICC05 extended chronology

Stephen P. Obrochta [a, *], Yusuke Yokoyama [a], Jan Morén [b], Thomas J. Crowley [c]

[a] University of Tokyo Atmosphere and Ocean Research Institute, 227-8564, Japan
[b] Neural Computation Unit, Okinawa Institute of Science and Technology, 904-0495, Japan
[c] Braeheads Institute, Maryfield, Braeheads, East Linton, East Lothian, Scotland EH40 3DH, UK

ARTICLE INFO

Article history:
Received 14 March 2013
Received in revised form
29 August 2013
Accepted 1 September 2013
Available online 19 September 2013

Keywords:
Chronology
Ice core
Sediment core
GICC05

ABSTRACT

Marine and lacustrine sediment-based paleoclimate records are often not comparable within the early to middle portion of the last glacial cycle. This is due in part to significant revisions over the past 15 years to the Greenland ice core chronologies commonly used to assign ages outside of the range of radiocarbon dating. Therefore, creation of a compatible chronology is required prior to analysis of the spatial and temporal nature of climate variability at multiple locations. Here we present an automated mathematical function that updates GISP2-based chronologies to the newer, NGRIP GICC05 age scale between 8.24 and 103.74 ka b2k. The script uses, to the extent currently available, climate-independent volcanic synchronization of these two ice cores, supplemented by oxygen isotope alignment. The modular design of the script allows substitution for a more comprehensive volcanic matching, once it becomes available. Usage of this function highlights on the GICC05 chronology, for the first time for the entire last glaciation, the proposed global climate relationships during the series of large and rapid millennial stadial-interstadial events.

1. Introduction

Radiocarbon measurements for the purpose of absolute age dating allow calculation of radiocarbon years to approximately 60 ka, the latter portion of Marine Isotope Stage (MIS) 4. However, calendar-year conversion is generally more limited, with the currently adopted IntCal09 calibration curve (Reimer et al., 2009) restricted to the past ~50 ka. Alternative calibration curves with longer temporal extent exist (Bard et al., 2004; Hughen et al., 2006), but the increasingly large uncertainty near the extreme radiocarbon detection range becomes problematic. Other direct dating methods are either generally inappropriate for sedimentary material (U-series) or only applicable to sediments that received special handling during core recovery (optically stimulated luminescence). While identification of tephra layers of known age allows indirect, absolute dating, the limited spatial distribution of volcanic material hinders the construction of a comprehensive, global tephrachronology (e.g., INTIMATE protocol, Lowe et al., 2008). Together, these factors have largely prevented the assignment of absolute age to marine and lacustrine sediments from an important interval of time that includes the last glacial inception (MIS 4/5 boundary) and the dispersal of modern humans out of Africa (e.g., Mellars, 2006) preceding the extinction of Neanderthals. This is especially the case for older sediment cores, to which the retroactive application of modern methods is often not possible due to the lack of pristine material.

To overcome these challenges when no other options are available, environmental and climate proxy records are often compared to a well-dated reference series that exhibits a distinguishable pattern of variability, allowing export of the reference chronology to clarify the relative deposition timing between strata at distant locations. The most common reference series are Greenland ice cores, which extend into the last interglacial period (MIS 5) and exhibit multiple, large-amplitude, abrupt warmings, commonly known as Dansgaard–Oeschger (D-O) Events (Dansgaard et al., 1993; Johnsen et al., 1992).

Bond et al. (1993) first demonstrated that last glacial North Atlantic sea surface temperature proxy records obtained from marine sediment cores exhibit a warming and cooling pattern comparable to Greenland. Since then, a large body of work indicates that these interstadial events are expressed as contemporaneous environmental fluctuations over a wide spatial area, centered on the North Atlantic Ocean and adjacent continental regions (Fletcher et al., 2010; Voelker, 2002; Bond et al., 1999), with far-reaching

* Corresponding author.
E-mail address: obrochta@aori.u-tokyo.ac.jp (S.P. Obrochta).

1871-1014/$ – see front matter © 2013 Elsevier B.V. All rights reserved.
http://dx.doi.org/10.1016/j.quageo.2013.09.001

connections to more distal areas via oceanic and atmospheric circulation changes (e.g., Anderson et al., 2009; Denton et al., 2010; Broecker et al., 2010; Yokoyama et al., 2001; Yokoyama and Esat, 2011). The coeval timing of these variations is supported by radiocarbon dating from the North Atlantic (e.g., Shackleton et al., 2004) and Arabian Sea (Schulz et al., 1998), as well as by U-series dating of Chinese speleothems.

The age of the ice in Greenland cores may be determined though the summing of annually deposited snow layers with a similar accuracy to radiocarbon dating. For example at 50,000 years ago, the Maximum Counting Error (MCE) (Rasmussen et al., 2006; Andersen et al., 2006) of the North GRIP (NGRIP) ice core results in an approximately $\pm$1000 year uncertainty (1σ) (Svensson et al., 2008), which is comparable to that for the same interval of IntCal09, prior to the addition of measurement error. Therefore, the combination of high precipitation rates in Greenland with the large spatial extent of the synchronous temperature changes provides a powerful tool for assigning ages that would otherwise be unknown.

However, there have been significant revisions to the Greenland ice core chronology over the past 15 years, with large discrepancies existing in the ages of the deeper sections of the different cores (Southon, 2004). Therefore, many of the published sediment core age models are incompatible. The largest offsets, up to 4000 years, exist between the early-glacial section of the GISP2 and NGRIP ice cores, which is the exact interval that radiocarbon is no longer available. Up until 2005, the Meese/Sowers 1994 (M/S94) timescale for the GISP2 ice core was the most widely used reference chronology. It is based on layer counting to 2431 m (50 ka) (Meese et al., 1994, 1997) below which the $\delta^{18}O$ of oxygen in trapped bubbles was astronomically tuned (Bender et al., 1994).

Subsequently, comparison to more recent work has highlighted an inconsistent climate–accumulation relationship imparted to GISP2 by M/S94 (e.g., Svensson et al., 2008) (Supplemental Fig. 1), and the virtually complete NGRIP ice core has since replaced GISP2 as the preferred reference for paleoenvironmental reconstructions of the last glaciation. Counting of NGRIP annual layers based on electrical conductivity measurements (ECM), continuous flow analysis (CFA), and visual stratigraphy from 14.8 to 60 ka constitutes the entire last glacial interval of the Greenland Ice Core Chronology 2005 (GICC05) timescale (Svensson et al., 2008, 2006; Andersen et al., 2006). GICC05 ages from 7.9 to 14.8 ka were obtained through ECM and CFA from both NGRIP and GRIP (Rasmussen et al., 2006), and the most recent interval of GICC05, from 0 to 7.9 ka, relies on annual layers expressed in the $\delta^{18}O$ and δD records from NGRIP, GRIP, and DYE-3 (Vinther et al., 2006). The deepest interval of NGRIP was dated to 123 ka by applying the ss09sea flow model with a $-$705 year shift ("GICC05modelext") (Wolff et al., 2010).

Here we present a mathematical function for automating the conversion of M/S94-based sediment core age models to GICC05modelext using either the Matlab or Octave (free, open source version of Matlab) high-level numerical computational languages, or the Python high-level programming language. This function will facilitate immediate comparison of older and newer data, which is required prior to attempting regional synthesis of early glacial climate records. This script implicitly uses the original authors' own tie points to the Greenland ice core record. Therefore, as described by Blaauw (2012), the uncertainties and limitations in the correlation procedures of the original authors must be considered. There are likely cases in the literature of over-enthusiastic "tuning" to Greenland, and the user should employ caution prior to interpretation following conversion to GICC05modelext to avoid circular inference. When possible, the original radiocarbon dates and tie points should be critically re-evaluated (e.g., Obrochta et al., 2012).

2. Methods

The conversion of M/S94-based chronologies to GICC05 may be performed online at http://paleo10.org/g2n or offline using a Matlab/Octave function or Python script. The offline versions consist of a conversion script (Supplemental Online Material) and a corresponding data file that contains the depth match points (synchronization lookup table) between the GISP2 and NGRIP $\delta^{18}O$ records. A separate data file simplifies script maintenance and the incorporation of future improvements, such as work currently in preparation including 1) a more comprehensive volcanic synchronization spanning the entire last glaciation (personal communication, Inger Seierstad and Sune Olander Rasmussen) and 2) an ice flow model to solve an inverse problem for improved age estimation between the volcanic match points (personal communication, Jessica Lundin and Ralf Greve).

The Matlab/Octave function is intended as a tool for use within an interactive Matlab or Octave environment, or for use within user-created analysis applications. The Python script is a standalone application and designed to work on any system with minimal third-party software requirements beyond Python itself. The online tool is powered by the Python script.

The output ages are based on GICC05modelext and relative to the number of calendar kiloyears before AD 2000 (i.e., kiloyears "b2k"), as opposed to before AD 1950 (i.e., "BP"). Dates outside of the conversion range of 8.24–103.74 ka b2k are not adjusted except for conversion to the b2k scale. This method is appropriate only for a time series with an age model derived from correlation to the GISP2 ice core with the M/S94 chronology. The data file version and synchronization references are also returned upon script execution.

2.1. Ice core synchronization

The initial version of the synchronization lookup table incorporates all the climate-independent synchronization points currently available. These are extensive volcanic match points from 8.24 to 32.48 ka b2k (Rasmussen et al., 2006, 2008), match points for the Toba mega-eruption from 74.06 to 76.04 ka b2k, as well as three smaller eruptions from 40.91 to 41.25 ka b2k during the Laschamp geomagnetic excursion (Svensson et al., 2012). These are supplemented by alignment of the $\delta^{18}O$ records from 33.60 to 40.08 and 76.24 to 103.74 ka b2k.

For $\delta^{18}O$ alignment, we used the 20-year sampled GICC05modelext timescale (http://www.iceandclimate.nbi.ku.dk/data/), which incorporates the ss09sea flow model (with a 705 year offset) from 60.2 to 123 ka ($n = 6114$). First, high-frequency variability was removed from the NGRIP $\delta^{18}O$ data by subtraction of a 500-year Gaussian high-pass filter. Then, this filtered record was compared in the depth domain to the much lower resolution GISP2 ($n = 1390$) $\delta^{18}O$ record, and individual warm events between Greenland Interstadial (GI) 6 and Greenland Interstadial (GI) 23 were aligned (Fig. 1). Warm events prior to GI23 were not aligned because $\delta^{18}O$ variations at these depths in GISP2 are difficult to interpret and unequivocally link to NGRIP.

This corresponds to the interval from 8.22 to 100.26 ka BP on the GISP2 M/S94 chronology and constitutes the maximum update interval range when no radiocarbon dates are specified. After conversion to the GICC05modelext timescale, the update interval ranges from 8.24 to 103.74 ka b2k. Older ages are truncated, and younger ages are converted to the b2k scale.

2.2. Update script

The Matlab/Octave update script is executed via the *g2n* command and accepts two input arguments. The first, mandatory input

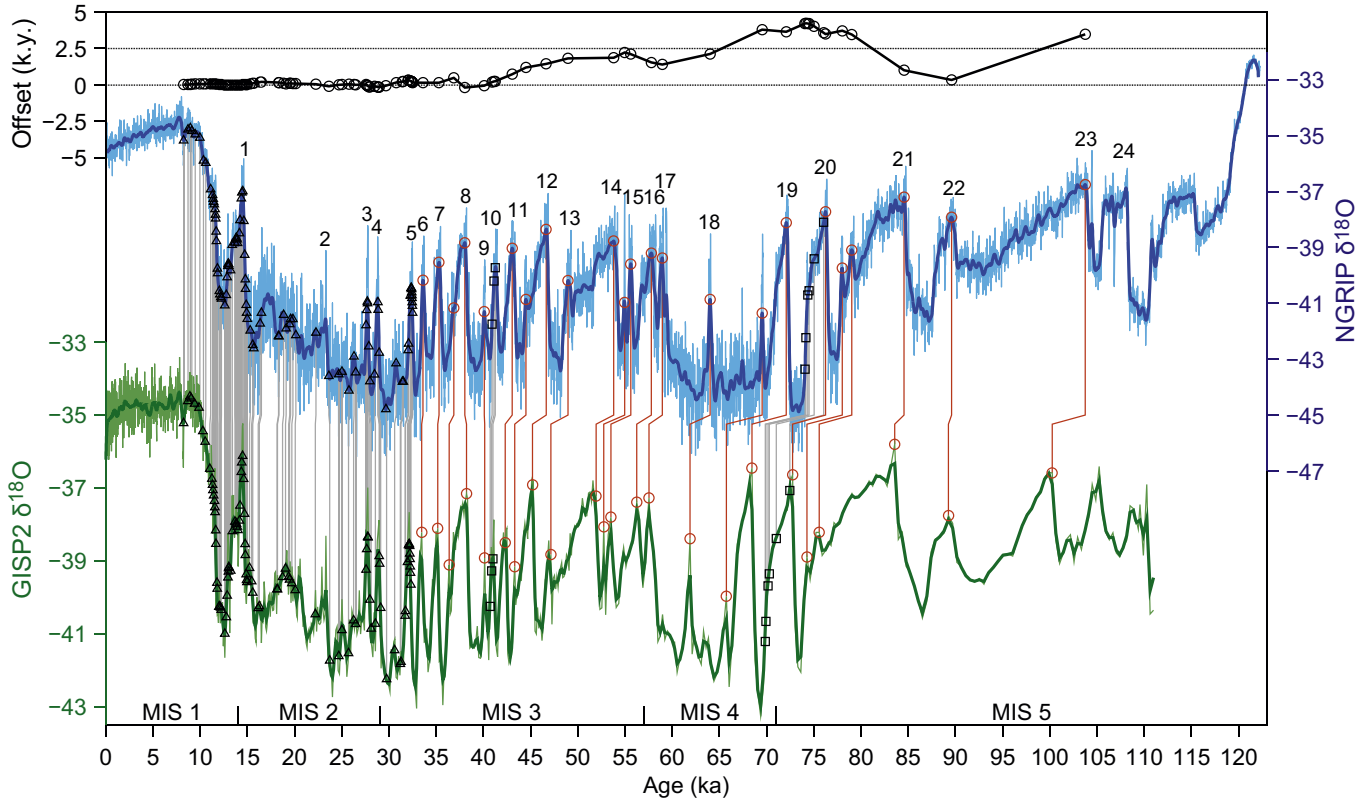

Fig. 1. The relative offset (top, black) between the NGRIP (middle, blue) and GISP2 (green, bottom) $\delta^{18}O$ records is shown with the match points used in the age update script. Volcanic tie points are represented as either triangles (Rasmussen et al., 2008, 2006) or squares (Svensson et al., 2012). The oxygen isotope tie points from this study are depicted as red circles. (For interpretation of the references to colour in this figure legend, the reader is referred to the web version of this article.)

argument is the target time series, formatted as a 2-column array of time values (x) in kiloyears BP (using the M/S94 chronology) and data values (y). The optional argument is the age of the oldest radiocarbon date (r), calibrated to calendar kiloyears BP (i.e., calibration distribution reduced to a midpoint, with error discarded). If it is specified and older than 8.22 ka BP, the range of the update interval is accordingly shortened. Otherwise, the script runs on the full update interval in the target series (8.22–100.26 ka BP). The output is a new 2-column array with remapped time and original data values. If x and y are separate vectors, the Matlab/Octave syntax becomes:

$g2n([x\,y], r)$

The Python script accepts a file (input.txt) of comma-separated or tab-delimited time and data values (in kiloyears BP as above), one pair per line. The output is a new comma-separated file with the remapped time and original data values. The user may optionally specify the radiocarbon cut-off date, the output file name, and years instead of kiloyears for the input time series. See the included documentation for details. With a 35.00 ka radiocarbon date, the syntax becomes:

python *g2n.py -c*35 input.txt

In both scripts the GISP2 and NGRIP synchronization is performed by first creating a new GISP2 depth scale consistent with the NGRIP scale through piecewise linear interpolation based on the depth match points. Next, the GICC05modelext timescale is transferred to the new GISP2 depth scale by looking up corresponding ages from the published NGRIP age–depth relationship, with intermediate values linearly interpolated between age–depth tie points. Following incorporation of the forthcoming flow model for assigning ages between tie points, the assignment of GICC05-modelext age to GISP2 will be performed based on the flow model output.

The new (GICC05modelext) and old (M/S94) GISP2 age vectors constitute the lookup table for updating the age model of the target time series to the GICC05 chronology. This is done by piecewise linear interpolation, taking into account the age of the oldest radiocarbon date, if specified. The output array is remapped to the GICC05modelext timescale from either 8.24 ka b2k or the age of the specified radiocarbon date, which ever is older, up to 103.74 ka b2k. Younger ages are returned unaltered except for conversion to the b2k scale. Older ages are discarded. Specification of a radiocarbon date within the limited intervals where GISP2 match points are "older" than NGRIP, as shown by negative offset in the top panel of Fig. 1, may result in an age reversal at the splice point of GICC05-based and absolutely-dated age data. In these cases, ages younger than the conversion interval are not imported; only GICC05-based ages are returned.

3. Results

Adjustments to the age model of the target series directly reflect the changes to the GISP2 ice core chronology, i.e., the offset displayed at the top of Fig. 1. Prior to ~38 ka, age changes are generally small (<500 years). From 38 to 40 ka, the interval subsequent to the Laschamp geomagnetic excursion and Heinrich Event 4 (H4), ages are shifted towards younger values. Farther back in time, prior to the occurrence of H4 and the Laschamp, ages are shifted to older values, with offset increasing to a maximum of ~4200 years at GS19, which reflects a change from 70.00 to 74.20 ka, subsequent to

the Toba Eruption. Offset then decreases to a relative minimum of ~340 years at ~90 ka. Identification of match points in the deeper layers of GISP2 is problematic. The last matchable point between the two ice cores is over 10,000 years older, at which the offset has again increased to ~3500 years. Finally, the GICC05 chronology results in a much more reasonable climate–accumulation relationship for GISP2 that is very similar to that of NGRIP (Supplemental Fig. 1). Accumulation consistently increases during each warming event in both ice cores.

4. Discussion

4.1. Additional age uncertainty

The age uncertainty from adapting GISP2 to GICC05 is in general much less than the NGRIP MCE. The maximum uncertainty in the volcanic ties of Rasmussen et al. (2008) is up to 1 m within a limited depth range of 1963.66–1990.98 m in GISP2. This corresponds to an average of 50 additional years of uncertainty, less than 10% of the MCE (~575 years). The uncertainty associated with the remainder of their volcanic match points typically adds only 5 additional years uncertainty, and no more than 15, which is generally about 1–2% of the MCE.

Rasmussen et al. (2008) further estimated that depth offset due to linear interpolation within longer sections lacking match points, while significant, does not exceed 0.5 m, corresponding to ~20 years within the intervals they examined. Such relatively minor age offsets are supported by preliminary flow model results that produce a similar GISP2 age profile as mathematical interpolation (Lundin et al., 2013). Thus, we interpret that the use of volcanic match points, with interpolation between these match points, is unlikely to introduce significant additional uncertainty to the target sediment core age models. However, linearly interpolating ice-core depth-age data lacks physical basis and is susceptible to over-fitting of noisy data, and climate reconstructions from linear interpolations, including accumulation-rate histories, can include spurious, non-physical artifacts that can be avoided with a physically based approach, including inverse methods with ice-flow forward models (personal communication, Jessica Lundin and Ralf Greve). Therefore, such a flow model, once available, will be incorporated into future versions of this program.

Greater uncertainty results from the $\delta^{18}O$ match points. This uncertainty is reflected in the depth range of the each individual warm event, which equates to as little as ~50 years for shorter-duration events, and up to 450 years for longer events at greater depths in GISP2. GI23, the oldest and most uncertain $\delta^{18}O$ match point, produces offset in excess of 1000 years from the preliminary volcanic matching. Excluding GI23, the use of $\delta^{18}O$ match points adds an average additional ~250 years of uncertainty. Comparison of warm event duration to MCE indicates that a 10% increase is appropriate. This is consistent with the 2σ range of variation in the mean offset of $\delta^{18}O$ and preliminary volcanic age profiles, ~10 ± 150 years up to GI22 (90 ka; Fig. 2).

4.2. Age model conversion examples

The script relies on the original authors' own depth tie points to the GISP2 ice core, changing only the age of those points to GICC05. Therefore, the phasing exhibited by the original series, relative to GISP2, will be preserved when comparing the updated series to NGRIP. To demonstrate this, several proxy records, each with previously published age models based on correlation to GISP2, are passed though our update function (Fig. 3). Included are 1) $\delta^{18}O$ and 2) CO_2 from the Byrd Antarctic ice core (Blunier and Brook, 2001; Ahn and Brook, 2007, 2008), 3) biogenic opal flux from the TN057-14PC4 Southern Ocean sediment core (Anderson et al., 2009), 4) magnetic susceptibility (MS) from the Arabian Sea 64 KL sediment core (Leuschner and Sirocko, 2000), 5) the mid-glacial portion of the sea surface salinity record (Ba/Ca ratio) from the coastal West African MD-03-2707 sediment core (Weldeab, 2012), and 6) the early glacial portion of the detrital carbonate (DC) ice-rafted debris (IRD) record from North Atlantic sediment core V23-81 (Bond et al., 1999). Supplemental Fig. 2.

The proxy records aligned to GISP2 by the original authors are not shown in Fig. 3. The Byrd ice core was aligned by synchronizing atmospheric methane concentrations. TN057-14 PC, MD03-2707, and 64 KL were aligned via foraminifer $\delta^{18}O$, and V23-81 was aligned using variations in the percentage of the left-coiling variety of the polar foraminifer *N. pachyderma*. The results are plotted with the DSDP Site 609 DC IRD record (Bond et al., 1999) using the updated chronology of Obrochta et al. (2012), the absolutely-dated Chinese speleothem $\delta^{18}O$ records from Sanbao and Hulu Caves (as shown in Wang et al., 2008), and NGRIP ice core $\delta^{18}O$ (Fig. 3). Conversion to GICC05modelext does not introduce any unreasonable changes in linear sedimentation rate (Supplemental Fig. 2).

During relatively cold Greenland stadials, large pulses of DC IRD at Sites 609 and V23-81 in the North Atlantic indicate the occurrence of Heinrich Events, surging of the Laurentide Ice Sheet, that contributed large volumes of freshwater to the North Atlantic (Bond et al., 1999). The reduced surface density drastically decreased the formation of deep water, reducing Atlantic meridional overturning circulation and diminishing northward heat

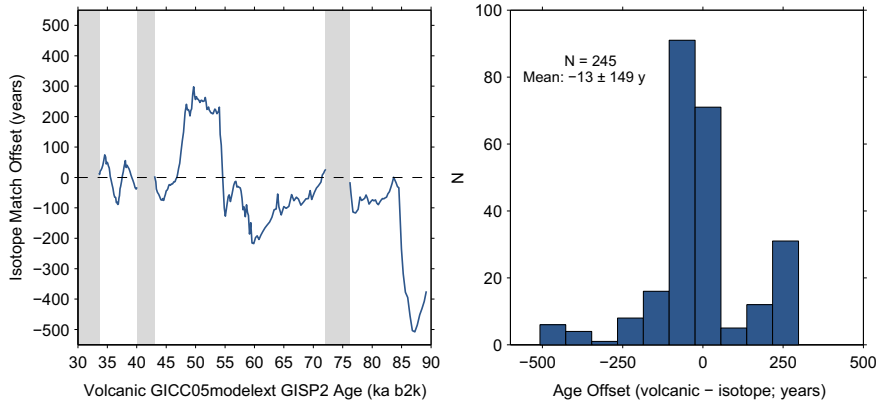

Fig. 2. Offset between comprehensive volcanic (in prep, Inger Seierstad and Sune Olander Rasmussen, Centre for Ice and Climate, Univ. of Copenhagen, Denmark) and isotope (this study) synchronization of GISP2 and NGRIP is shown in time (left) and as a distribution (right). Gray bars represent time intervals with available volcanic synchronization.

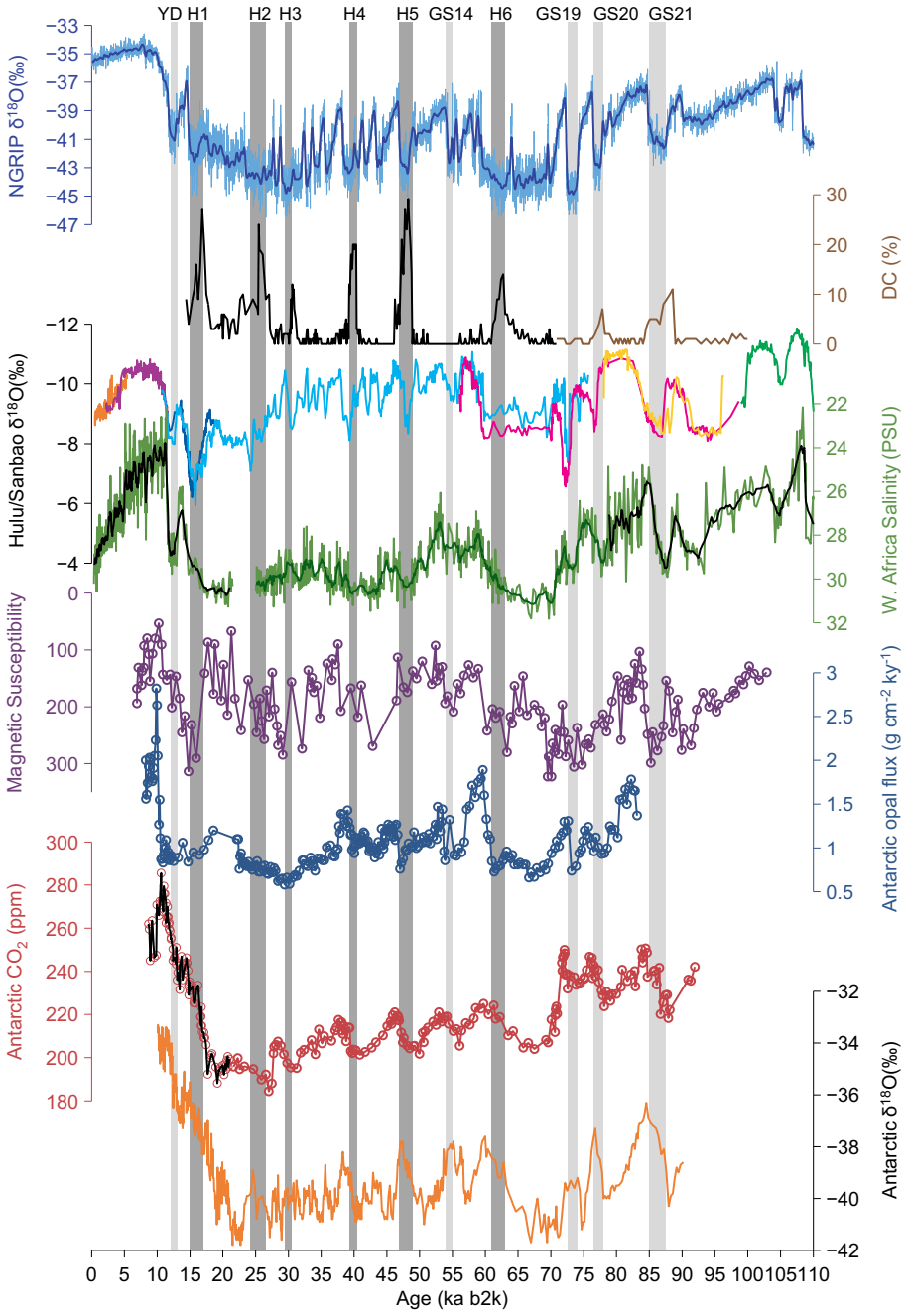

Fig. 3. Example application of conversion function. Shown for reference are the Greenland NGRIP ice core $\delta^{18}O$ (blue), North Atlantic detrital carbonate (DC) from Site 609 (Obrochta et al., 2012; Bond et al., 1999) (black), and the Chinese Sanbao and Hulu speleothem records (coloring after Wang et al. (2008)). Records converted to GICC05 using the script presented here are: the V23-81 North Atlantic DC record (brown) (Bond et al., 1999), the MD03-2707 West African sea surface salinity record (Weldeab, 2012) (green), the 64 KL Arabian Sea magnetic susceptibility (MS) (Leuschner and Sirocko, 2000) (purple), the TN057-14 PC opal flux (Anderson et al., 2009) (blue), and the Antarctic Byrd CO_2 (red) and $\delta^{18}O$ (orange) records (Ahn and Brook, 2007; Ahn and Brook, 2008). The portions drawn with thick black lines represent intervals that were independently converted to GICC05 and include, the youngest and oldest intervals of MD03-2707 (Weldeab et al., 2007) and the youngest portion of the Byrd CO_2 record (Pedro et al., 2011). (For interpretation of the references to colour in this figure legend, the reader is referred to the web version of this article.)

transport (Crowley, 1992). Antarctic ice core $\delta^{18}O$ indicates the balance of heat shifted towards the Southern Hemisphere (Blunier and Brook, 2001), with Northern Hemisphere cooling and expanded sea ice displacing latitudinal circulation belts to more southerly locations. Weak African, Indian, and East Asian summer monsoon events recorded at sites MD03-2707 and 64 KL, as well as by Chinese speleothems reflect this southward ITCZ shift (Leuschner and Sirocko, 2000; Weldeab, 2012; Wang et al., 2008). This is followed by increased upwelling in the Southern Ocean, reflected by high primary productivity and subsequent increased biogenic opal flux at Site TN057-14 PC (Anderson et al., 2009). Upwelling would have also ventilated CO_2 produced from microbial respiration of organic matter, as recorded in Antarctic ice cores.

Demonstrating the early- to mid-glacial bipolar "see-saw", first described by Crowley (1992), previously required converting NGRIP-based records (e.g., Weldeab et al., 2007) to GISP2-based chronologies (e.g., Weldeab, 2012). The use of our function now allows for interhemispheric comparison based on the GICC05modelext

chronology, using the original author's own age control points. Only the underlying chronology is changed. The above example displays, for the first time for the entire last glaciation, the proposed global climate relationship to rapid Northern Hemisphere climate change (e.g., Denton et al., 2010; Broecker et al., 2010; Yokoyama and Esat, 2011) on the most up-to-date Greenland ice core chronology.

5. Conclusions

An automated update script converts paleo time series from the GISP2-based M/S94 chronology to the GICC05modelext chronology over the interval between the early Holocene (or the age of the oldest radiocarbon date) and GI23, corresponding to 8.24 (8.22) to 103.74 (100.26) ka in the NGRIP (GISP2) ice core. The script is modular in design, allowing substitution of our $\delta^{18}O$-based matching for the more comprehensive volcanic matching, once available. When applied to appropriate records, relative phasing between the target time series and Greenland is preserved. Until incorporation of the volcanic synchronization currently in preparation, care should be used interpreting the significance of events in excess of 90 ka. This script allows for the creation of coherent chronologies to facilitate quantitative statistical analysis of spatial and temporal climate variability over large regions. An example application of this script highlights on the GICC05 chronology, for the first time for the entire last glaciation, the series and timing of events related to the large, Northern Hemisphere millennial climate perturbations.

Acknowledgments

This work was supported by JSPS Kakenhi 22101005 and the NEXT program GR031. Discussion with S.O. Rasmussen, K. Kawamura, R. Greve, and J. Lundin greatly improved this work. We thank Paul Hesse and an anonymous reviewer for helpful comments.

Editorial handling by: T. Higham

Appendix A. Supplementary data

Supplementary data related to this article can be found at http://dx.doi.org/10.1016/j.quageo.2013.09.001.

References

Ahn, J., Brook, E.J., 2007. Atmospheric CO_2 and climate from 65 to 30 ka B.P. Geophys. Res. Lett. 34 (10).

Ahn, J., Brook, E.J., 2008. Atmospheric CO_2 and climate on millennial time scales during the last glacial period. Science 322 (5898), 83–85.

Andersen, K.K., Svensson, A., Johnsen, S.J., Rasmussen, S.O., Bigler, M., Rthlisberger, R., Ruth, U., Siggaard-Andersen, M.-L., Peder Steffensen, J., Dahl-Jensen, D., Vinther, B.M., Clausen, H.B., 2006. The Greenland ice core chronology 2005, 15–42 ka. Part 1: constructing the time scale. Quatern. Sci. Rev. 25 (23–24), 3246–3257.

Anderson, R.F., Ali, S., Bradtmiller, L.I., Nielsen, S.H.H., Fleisher, M.Q., Anderson, B.E., Burckle, L.H., 2009. Wind-driven upwelling in the Southern ocean and the deglacial rise in atmospheric CO_2. Science 323 (5920), 1443–1448.

Bard, E., Ménot-Combes, G., Rostek, F., 2004. Present status of radiocarbon calibration and comparison records based on Polynesian corals and Iberian margin sediments. Radiocarbon 46 (3), 1189–1202.

Bender, M., Sowers, T., Dickson, M.-L., Orchardo, J., Grootes, P., Mayewski, P.A., Meese, D.A., 1994. Climate correlations between Greenland and Antarctica during the past 100,000 years. Nature 372 (6507), 663–666.

Blaauw, M., 2012. Out of tune: the dangers of aligning proxy archives. Quatern. Sci. Rev. 36 (0), 38–49.

Blunier, T., Brook, E.J., 2001. Timing of millennial-scale climate change in Antarctica and Greenland during the Last Glacial Period. Science 291 (5501), 109–112.

Bond, G.C., Broecker, W., Johnsen, S., McManus, J., Labeyrie, L., Jouzel, J., Bonani, G., 1993. Correlations between climate records from North-Atlantic sediments and Greenland Ice. Nature 365 (6442), 143–147.

Bond, G.C., Showers, W., Elliot, M., Evans, M.N., Lotti, R., Hajdas, I., Bonani, G., Johnsen, S., 1999. The North Atlantic's 1–2 kyr climate rhythm: relation to Heinrich events, Dansgaard/Oeschger cycles and the little ice age. In: Clark, P.U., Webb, R.S., Keigwin, L.d. (Eds.), Mechanisms of Global Climate Change at Millennial Time Scales. AGU, Washington D.C., pp. 35–58.

Broecker, W.S., Denton, G.H., Edwards, R.L., Cheng, H., Alley, R.B., Putnam, A.E., 2010. Putting the Younger Dryas cold event into context. Quatern. Sci. Rev. 29 (9–10), 1078–1081.

Crowley, T.J., 1992. North Atlantic deep water cools the Southern Hemisphere. Paleoceanography 7 (4), 489–497.

Dansgaard, W., Johnsen, S.J., Clausen, H.B., Dahl-Jensen, D., Gundestrup, N.S., Hammer, C.U., Hvidberg, C.S., Steffensen, J.P., Sveinbjornsdottir, A.E., Jouzel, J., Bond, G., 1993. Evidence for general instability of past climate from a 250-kyr ice-core record. Nature 364 (6434), 218–220.

Denton, G.H., Anderson, R.F., Toggweiler, J.R., Edwards, R.L., Schaefer, J.M., Putnam, A.E., 2010. The last glacial termination. Science 328 (5986), 1652–1656.

Fletcher, W.J., Sánchez Goñi, M.F., Allen, J.R.M., Cheddadi, R., Combourieu-Nebout, N., Huntley, B., Lawson, I., Londeix, L., Magri, D., Margari, V., Müller, U.C., Naughton, F., Novenko, E., Roucoux, K., Tzedakis, P.C., 2010. Millennial-scale variability during the last glacial in vegetation records from Europe. Quatern. Sci. Rev. 29 (21–22), 2839–2864.

Hughen, K., Southon, J., Lehman, S., Bertrand, C., Turnbull, J., 2006. Marine-derived ^{14}C calibration and activity record for the past 50,000 years updated from the Cariaco Basin. Quatern. Sci. Rev. 25 (23–24), 3216–3227.

Johnsen, S.J., Clausen, H.B., Dansgaard, W., Fuhrer, K., Gundestrup, N., Hammer, C.U., Iversen, P., Jouzel, J., Stauffer, B., Steffensen, J.P., 1992. Irregular glacial interstadials recorded in a new Greenland ice core. Nature 359 (6393), 311–313.

Leuschner, D.C., Sirocko, F., 2000. The low-latitude monsoon climate during Dansgaard–Oeschger cycles and Heinrich events. Quatern. Sci. Rev. 19 (1–5), 243–254.

Lowe, J.J., Rasmussen, S.O., Björck, S., Hoek, W.Z., Steffensen, J.P., Walker, M.J.C., Yu, Z.C., 2008. Synchronisation of palaeoenvironmental events in the North Atlantic region during the last termination: a revised protocol recommended by the INTIMATE group. Quatern. Sci. Rev. 27 (1–2), 6–17.

Lundin, J.M.D., Greve, R., Rasmussen, S.O., Seierstad, I., Waddington, E.D., 2013. An Updated Chronology and Inference of Climate Evolution for the GISP2 Ice Core from Summit, Greenland, Chiba, Japan. http://www2.jpgu.org/meeting/2013/session/PDF/A-CC33/ACC33-12_E.pdf.

Meese, D.A., Alley, R.B., Fiacco, R.J., Germani, M.S., Gow, A.J., Grootes, P.M., Illing, M., Mayewski, P.A., Morrison, M.C., Ram, M., Taylor, K.C., Yang, Q., Zielinski, G.A., 1994. Preliminary Depth-agescale of the GISP2 Ice Core, p. 66. Special CRREL Report 94-1.

Meese, D.A., Gow, A.J., Alley, R.B., Zielinski, G.A., Grootes, P.M., Ram, M., Taylor, K.C., Mayewski, P.A., Bolzan, J.F., 1997. The Greenland Ice Sheet Project 2 depth-age scale: methods and results. J. Geophys. Res. 102 (C12), 26411–26423.

Mellars, P., 2006. Why did modern human populations disperse from Africa ca. 60,000 years ago? A new model. Proc. Natl. Acad. Sci. 103 (25), 9381–9386.

Obrochta, S.P., Miyahara, H., Yokoyama, Y., Crowley, T.J., 2012. A re-examination of evidence for the North Atlantic "1500-year cycle" at Site 609. Quatern. Sci. Rev. 55, 23–33.

Pedro, J.B., van, O.,T.D., Rasmussen, S.O., Morgan, V.I., Chappellaz, J., Moy, A.D., Masson-Delmotte, V., Delmotte, M., 2011. The last deglaciation: timing the bipolar seesaw. Clim. Past 7 (2), 671–683.

Rasmussen, S.O., Andersen, K.K., Svensson, A.M., Steffensen, J.P., Vinther, B.M., Clausen, H.B., Siggaard-Andersen, M.-L., Johnsen, S.J., Larsen, L.B., Dahl-Jensen, D., Bigler, M., Röthlisberger, R., Fischer, H., Goto-Azuma, K., Hansson, M.E., Ruth, U., 2006. A new Greenland ice core chronology for the last glacial termination. J. Geophys. Res. Atmos. 111 (D6).

Rasmussen, S.O., Seierstad, I.K., Andersen, K.K., Bigler, M., Dahl-Jensen, D., Johnsen, S.J., 2008. Synchronization of the NGRIP, GRIP, and GISP2 ice cores across MIS 2 and palaeoclimatic implications. Quatern. Sci. Rev. 27 (1–2), 18–28.

Reimer, P.J., Baillie, M.G.L., Bard, E., Bayliss, A., Beck, J.W., Blackwell, P.G., BronkRamsey, C., Buck, C.E., Burr, G.S., Edwards, R.L., Friedrich, M., Grootes, P.M., Guilderson, T.P., Hajdas, I., Heaton, T.J., Hogg, A.G., Hughen, K.A., Kaiser, K.F., Kromer, B., McCormac, F.G., Manning, S.W., Reimer, R.W., Richards, D.A., Southon, J.R., Talamo, S., Turney, C.S.M., vanderPlicht, J., Weyhenmeyer, C.E., 2009. IntCal09 and Marine09 radiocarbon age calibration curves, 0–50,000 years cal BP. Radiocarbon 51 (4), 1111–1150.

Schulz, H., von Rad, U., Erlenkeuser, H., 1998. Correlation between Arabian sea and Greenland climate oscillations of the past 110,000 years. Nature 393 (6680), 54–57.

Shackleton, N.J., Fairbanks, R.G., Chiu, T.-, Parrenin, F., 2004. Absolute calibration of the Greenland time scale: implications for Antarctic time scales and for [Delta] 14C. Quatern. Sci. Rev. 23 (14–15), 1513–1522.

Southon, J., 2004. A radiocarbon perspective on Greenland ice-core chronologies; can we use ice cores for (super 14) C calibration? Radiocarbon 46 (3), 1239–1259.

Svensson, A., Andersen, K.K., Bigler, M., Clausen, H.B., Dahl-Jensen, D., Davies, S.M., Johnsen, S.J., Muscheler, R., Rasmussen, S.O., Röthlisberger, R., Peder Steffensen, J., Vinther, B.M., 2006. The Greenland Ice Core Chronology 2005, 15–42 ka. Part 2: comparison to other records. Quatern. Sci. Rev. 25 (23–24), 3258–3267.

Svensson, A., Andersen, K.K., Bigler, M., Clausen, H.B., Dahl-Jensen, D., Davies, S.M., Johnsen, S.J., Muscheler, R., Parrenin, F., Rasmussen, S.O., Röthlisberger, R., Seierstad, I., Steffensen, J.P., Vinther, B.M., 2008. A 60,000 year Greenland stratigraphic ice core chronology. Clim. Past 4 (1), 47–57.

Svensson, A., Bigler, M., Blunier, T., Clausen, H.B., Dahl-Jensen, D., Fischer, H., Fujita, S., Goto-Azuma, K., Johnsen, S.J., Kawamura, K., Kipfstuhl, S., Kohno, M.,

Parrenin, F., Popp, T., Rasmussen, S.O., Schwander, J., Seierstad, I., Severi, M., Steffensen, J.P., Udisti, R., Uemura, R., Vallelonga, P., Vinther, B.M., Wegner, A., Wilhelms, F., Winstrup, M., 2012. Direct linking of Greenland and Antarctic ice cores at the Toba eruption (74 ka BP). Clim. Past 9 (2), 749–766.

Vinther, B.M., Clausen, H.B., Johnsen, S.J., Rasmussen, S.O., Andersen, K.K., Buchardt, S.L., Dahl-Jensen, D., Seierstad, I.K., Siggaard-Andersen, M.-L., Steffensen, J.P., Svensson, A., Olsen, J., Heinemeier, J., 2006. A synchronized dating of three Greenland ice cores throughout the Holocene. J. Geophys. Res. Atmos. 111 (D13), D13102.

Voelker, A.H.L., 2002. Global distribution of centennial-scale records for Marine Isotope Stage (MIS) 3: a database. Quatern. Sci. Rev. 21 (10), 1185–1212.

Wang, Y., Cheng, H., Edwards, R.L., Kong, X., Shao, X., Chen, S., Wu, J., Jiang, X., Wang, X., An, Z., 2008. Millennial- and orbital-scale changes in the East Asian monsoon over the past 224,000 years. Nature 451 (7182), 1090–1093.

Weldeab, S., 2012. Bipolar modulation of millennial-scale West African monsoon variability during the last glacial (75,000–25,000 years ago). Quatern. Sci. Rev. 40 (0), 21–29.

Weldeab, S., Lea, D.W., Schneider, R.R., Andersen, N., 2007. 155,000 years of West African monsoon and ocean thermal evolution. Science 316 (5829), 1303–1307.

Wolff, E.W., Chappellaz, J., Blunier, T., Rasmussen, S.O., Svensson, A., 2010. Millennial-scale variability during the last glacial: the ice core record. Quatern. Sci. Rev. 29 (21–22), 2828–2838.

Yokoyama, Y., Esat, T.M., 2011. Global climate and sea level: enduring variability and rapid fluctuations over the past 150,000 years. Oceanography 24 (2).

Yokoyama, Y., Esat, T.M., Lambeck, K., 2001. Coupled climate and sea-level changes deduced from Huon Peninsula coral terraces of the last ice age. Earth Planet. Sci. Lett. 193 (3–4), 579–587.